

# Photophysical and electrochemical properties of *meso*-tetrathien-2'-yl porphyrins compared to *meso*-tetraphenylporphyrin

Jessica S. O'Neill<sup>a,1</sup>, Nicola M. Boyle<sup>a,b,1</sup>, Thayse Marques Passos<sup>c</sup>, Katharina Heintz<sup>a</sup>, Wesley R. Browne<sup>b,\*</sup>, Brid Quilty<sup>c,\*</sup>, Mary T. Pryce<sup>a,\*</sup>

<sup>a</sup> School of Chemical Sciences, Dublin City University, Dublin 9, Ireland

<sup>b</sup> Stratingh Institute for Chemistry, University of Groningen, Nijenborgh 4, 9747AG Groningen, the Netherlands

<sup>c</sup> School of Biotechnology, Dublin City University, Dublin 9, Ireland

## ARTICLE INFO

### Keywords:

Porphyrin  
Thiophene  
Photophysical  
Electrochemistry  
Raman  
Singlet oxygen  
Antimicrobial

## ABSTRACT

A series of novel tetra-*meso*-thien-2-yl porphyrins were synthesised, and the effect of the variation in the thienyl group on the photophysical properties were studied. Ground and excited state UV–vis absorption, steady-state and time-resolved emission, resonance Raman spectroscopy, and cyclic voltammetry, were used to establish the extent of electronic communication between the central Zn(II) porphyrin ring and the various *meso*-substituent groups. The properties of these novel thienyl porphyrins were compared to zinc tetraphenylporphyrin (ZnTPP), to elucidate the effect of the position and number of thienyl rings. The photochemically-driven antimicrobial activity of zinc(II)-5,10,15,20-tetra(thien-2'-yl)porphyrin (ZnThPP) as a coating, was established against both Gram-positive and Gram-negative bacteria, and compared to ZnTPP. Visible irradiation of the porphyrins results in a significant antimicrobial response.

## 1. Introduction

Thienyl-decorated porphyrins and similar macrocycles can have unique properties with the thienyl groups tuning spectroscopic properties.<sup>1–3</sup> Thienyl-substituted porphyrins have applications in areas such as CO<sub>2</sub> reduction, the fabrication of dye-sensitised solar cells (DSSCs) and various biological applications.<sup>4–8</sup> *Meso*-thienyl porphyrins are potentially suitable for antimicrobial and anticancer applications due to their ability to generate singlet oxygen, and to intercalate with DNA.<sup>5–10</sup>

Zinc tetraphenylporphyrin (ZnTPP) is often used as a benchmark to compare other novel dyes.<sup>11</sup> Both electron-withdrawing groups and electron-donating groups have a strong influence on the electronic behaviour of the porphyrin, with *meso*-thienyl substituents displaying strong electron donation towards the porphyrin core.<sup>12–14</sup> Enhanced resonance between the *meso*-substituents and the porphyrin macrocycle results in improved  $\pi$ -conjugation.<sup>1</sup> Incorporation of thienyl groups at the *meso* position results in a bathochromic shift in both the Soret and Q bands due to enhanced electronic and vibronic communication.<sup>1,6,14–18</sup> The Soret band for tetra-5,10,15,20-(5'-methylthien-2'-yl)porphyrin displayed a 15 nm red shift compared to the tetraphenyl analogue,

together with positive solvatochromic behaviour which originates from the extended conjugation.<sup>19</sup> Replacement of one thienyl unit with a phenyl on a porphyrin resulted in hypsochromic shifts of both absorption and fluorescent bands, indicating decreased conjugation between the porphyrin macrocycle and thienyl units.<sup>20</sup> Planar *meso*-substituents with respect to the porphyrin result in stronger  $\pi$ -conjugation in comparison to orthogonal orientation, such as phenyl groups.<sup>14,17,21</sup>

Thienyl-containing macrocycles have been reported to exhibit reduced excited state lifetimes and enhanced triplet crossing efficiency when compared to phenyl substituents.<sup>22–24</sup> Ambre et. al, reported a reduction of excited state lifetimes proportional to the addition of thiophene units, from 2.00 ns to 0.88 ns as the number of thiophene units increased from one to three.<sup>25</sup> The presence of sulphur enhances the rate of intersystem crossing due to spin–orbit coupling, leading to a reduction in fluorescence quantum yield by up to 10%.<sup>1,16,20,21,23</sup> A decrease in the HOMO-LUMO energy gap was reported by Bhyrappa and Bhavana, when the point of substitution of the thienyl group was varied (from tetra(thien-2-yl)porphyrin to tetra(thien-3-yl)porphyrin.<sup>26</sup> The changes observed in the UV–vis spectra and redox potentials were attributed to the inductive effects of the thienyl groups.

\* Corresponding authors.

E-mail addresses: [w.r.browne@rug.nl](mailto:w.r.browne@rug.nl) (W.R. Browne), [brid.quilty@dcu.ie](mailto:brid.quilty@dcu.ie) (B. Quilty), [mary.pryce@dcu.ie](mailto:mary.pryce@dcu.ie) (M.T. Pryce).

<sup>1</sup> J. O'Neill and N. Boyle contributed equally to this work.

Modified thienyl porphyrins have displayed improved performance for cellular inactivation within photoactivated chemotherapy (PACT) applications.<sup>9,27</sup> Thienyl-decorated porphyrins have been reported to cleave DNA through a  $^1\text{O}_2$ -mediated mechanism.<sup>6</sup> These systems have also been used to bind DNA and as light-activated antimicrobial agents towards both *E. coli* and *S. aureus*.<sup>28</sup> Modification at either the meta- or beta- substituents can potentially increase the generation of  $^1\text{O}_2$ .<sup>29-31</sup> *Meso*-modifications can impact spectral characteristics, electrochemical and phototoxic properties.<sup>32,33</sup> Porphyrins can be immobilized, which offers many advantages for use in practical applications, such as coatings. Beyond tetra-substituted porphyrins, both A3B and A2B2 thienyl porphyrins have been developed towards immobilization or enhanced DNA groove binding.<sup>28,34</sup> Furthermore, they can be easily recovered and reused in water purification, thus providing both environmental and economic benefits.<sup>35</sup> Immobilization allows for easy isolation of the reaction products from the photosensitizer in photochemical synthesis thus allowing flexibility in fine chemical synthesis.<sup>36</sup>

The first investigation into porphyrins for the photodynamic inactivation of microbial cells utilized hematoporphyrin (HP) against Gram-positive and Gram-negative bacteria.<sup>37</sup> The photochemical impact was investigated using prokaryotes, with high sensitivity for the Gram-positive strains identified. In contrast, Gram-negative strains were less sensitive which was ascribed to their outer membrane containing lipopolysaccharide (LPS).<sup>37</sup> This layer imparts protection against singlet oxygen and oxyradicals, which are generated extracellularly. The barrier is especially effective due to the extremely short lifetime of  $^1\text{O}_2$  in water.<sup>38</sup> Lacking an LPS membrane, Gram-positive bacteria, have a more porous cell membrane and penetration of ROS is easier.<sup>39,40</sup>

Differences in response between Gram-positive and Gram-negative bacteria have been attributed to differences in their outer cell layers. The outer layers of Gram-positive cells comprising peptidoglycan and lipoteichoic acid are relatively porous to porphyrins while the cell wall of Gram (-) cells are rich in negatively charged LPS layer which hinders entry to the cell by neutral and anionic porphyrins.<sup>41</sup> Other studies have shown that Zn porphyrin-based photosensitizers can be effective against Gram-positive and Gram-negative bacteria. Alenezi et al. found that Zn porphyrin-based photosensitizers were effective against the Gram-negative bacterium *E. coli*.<sup>29</sup> Rahimi et al. studied bacterial inactivation by 5,10,15,20-tetrakis(4-nitrophenyl)porphyrin (TNPP) and its zinc analogue (ZnTNPP) on the Gram-negative bacterium *Pseudomonas aeruginosa* and the Gram-positive bacterium *Bacillus subtilis* under visible light irradiation.<sup>42</sup> Using the plate dilution method, the minimum inhibitory concentration (MIC) was investigated and found that bacteria growth was inhibited. Mosinger et al. reported the antibacterial activity of immobilized zinc tetraphenylporphyrin (ZnTPP) and zinc phthalocyanine (ZnPc) on polyurethane nanofabrics.<sup>43</sup> *Escherichia coli* DH5 $\alpha$

containing plasmid pGEM11Z showed no growth following illumination with a cold white light for 30 min. These results indicated that the photosensitizer-doped nanofabrics produced enough  $^1\text{O}_2$  to kill bacteria on their surfaces.

In this study, a range of thienyl porphyrins (see Fig. 1) were synthesized and their photophysical characteristics were compared. The novel porphyrins were compared to ZnTPP and the porphyrins zinc tetrathien-2'-ylporphyrin (ZnTThP) and zinc tetrathien-3'-ylporphyrin (ZnT3ThP). We report the spectroscopic, photophysical, and redox properties of symmetrical Zn(II) porphyrins with various thiophene-based *meso*-substituents, together with preliminary antibacterial studies of zinc tetraphenylporphyrin and zinc tetrathien-2'-ylporphyrin when coated onto glass beads.

## 2. Experimental section

The synthesis and characterization of the porphyrins studied here are described in the Supporting Information. UV-vis absorption and emission spectra were recorded in spectroscopic grade dichloromethane (Aldrich) at room temperature on an Agilent Technologies 8453 diode array spectrophotometer, using 10 mm quartz cuvettes. Steady-state emission spectra were recorded at room temperature on an LS50B luminescence spectrophotometer, equipped with a Hamamatsu R928 PMT detector, interfaced with Elonex PC466 using Perkin-Elmer FL WinLab.

**Transient absorption (TA)** spectral data were obtained using pulsed excitation at 355 and 532 nm in toluene under 1 atm of argon at room temperature with a typical sample absorbance of 0.8 ( $\pm 0.1$ ) at the wavelength of excitation corresponding to concentrations of less than 1  $\mu\text{M}$ . All transient species we observed were independent of excitation wavelength and formed within the lifetime of the laser pulse (ca. 10 ns). The TA difference spectra are attributed to the generation of the lowest  $^3(\pi - \pi^*)$  porphyrin triplet excited state. All transient signals recorded in this study fit well with mono-exponential kinetics indicating unimolecular decays at this concentration.

**Cyclic voltammograms** were recorded using a CH instrument model 600a electrochemical workstation at a scan rate of 0.1  $\text{V s}^{-1}$ , at a 2 mm diameter Teflon shrouded glassy carbon working electrode, with a platinum wire auxiliary electrode and a saturated calomel reference electrode, with spectrophotometric grade dichloromethane (Aldrich) and 0.1 M TBAPF<sub>6</sub> (Fluka Chemicals). Solutions were deoxygenated by purging with nitrogen and held under a blanket of nitrogen during experiments.

**Raman spectra** were recorded at 355 nm (10 mW Cobolt Lasers), 400.8 nm (50 mW at source, Power Technology), 449 nm (35 mW at source, Power Technology), and 473 nm (100 mW at source, Cobolt

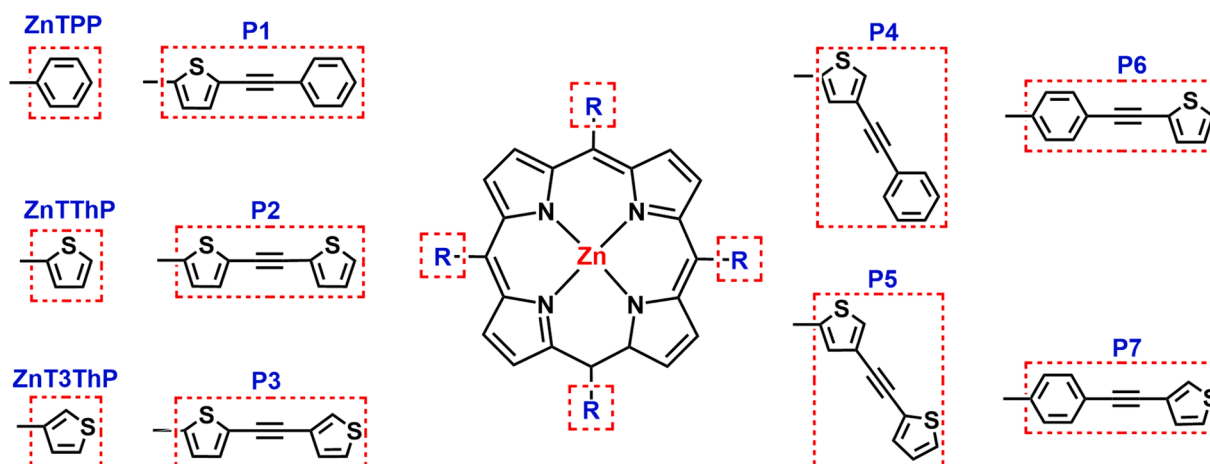


Fig. 1. Structures of the *meso*-Zn(II)thien-2'-ylporphyrins and *meso*-Zn(II)phenylporphyrins prepared for this study.

Lasers) in dichloromethane solutions in quartz cuvettes in a 180° backscattering arrangement was used with a 5 cm diameter plano-convex lens ( $f = 6$  cm) used for focusing the laser and collecting Raman scattering. The collimated Raman scattering was passed through an appropriate long pass filter (Semrock) and focused by a second 5 cm diameter plano-convex lens ( $f = 6$  cm) into a Shamrock 300i spectrograph (Andor Technology) with a 1200 L/mm grating blazed at 500 nm or 2400 L/mm blazed at 400 nm and acquired with an idus-DV420A-BU2 CCD camera (Andor Technology). The slit width was set to 10 or 20  $\mu\text{m}$ . Each spectrum was accumulated, typically 20 times with 5 s acquisition time, resulting in a total acquisition time of 1–2 min per spectrum. Data were recorded and processed using Solis (Andor Technology) and Spectragryph with spectral calibration performed using the Raman spectrum of acetonitrile/toluene 50:50 (v:v). The UV–vis absorption spectra recorded before and after each measurement verified that changes had not taken place during the measurement. Multipoint baseline correction was performed for all spectra. The concentrations used for resonance Raman studies were ca. 10–100  $\mu\text{M}$  for all samples depending on excitation wavelength and molar absorptivity.

**Singlet Oxygen** quantum yields were determined from its phosphorescence at 1270 nm using a 512-element InGaAs diode array detector (Andor idus-InGaAs) coupled to a shamrock163 spectrograph (Andor Technology) via a round-to-line bundle of fibres (3, 105  $\mu\text{m}$  diameter), with the sample held in a Thorlabs cuvette holder (CVH100/M) with long pass filter to reject excitation light and scatter, and with excitation at 90°. The  $^1\text{O}_2$  quantum yields of the porphyrins **P1–P7** were determined in dichloromethane relative to the reference compound, **ZnTPP** ( $\Phi = 0.68$ ) using equation (1), where  $\Phi$  is the quantum yield for singlet oxygen generation,  $G$  is the integrated area under the  $^1\text{O}_2$  emission and  $A$  is the absorbance at the excitation wavelength. Superscripts and subscripts of REF and S correspond to the reference and sample, respectively. In all cases, the  $^1\text{O}_2$  emission spectra were measured by excitation at 430 nm with the absorbance set at less than 0.2 to minimize the re-absorption of emitted light.

$$\Phi_S = \Phi_{\text{REF}} \frac{G_S}{G_{\text{SAM}}} \frac{A_{\text{REF}}}{A_S}$$

**Antimicrobial activity** of **ZnTThP** was assessed using *Escherichia coli* DSM 1103 and *Staphylococcus aureus* DSM 799. The bacteria were cultured aerobically overnight in 10 ml of nutrient broth at 150 rpm and 35 °C. These bacteria cultures were washed twice (4000 rpm for 20 min) and re-suspended in 10 ml of PBS. The optical density was adjusted accordingly to give  $1 \times 10^7$  CFU/ml (colony forming units) in PBS. Glass beads of 3.00 mm diameter (Merck, Germany) were used as a support to immobilize the porphyrins. Two grams of glass beads were added to a solution containing 2.00 mg of porphyrin per 2 ml solvent ( $\text{CH}_2\text{Cl}_2$ ). The solvent was removed under a stream of nitrogen, leading to the beads coated with porphyrin.

The coated glass beads were placed in glass petri dishes (60 x15mm) and covered with 9.9 ml PBS. 100  $\mu\text{l}$  of bacterial suspension was added to each petri dish to give a final concentration of  $10^5$  CFU/mL. The plates were agitated and irradiated under a dichromatic lamp (430 and 660 nm) for 180 min. An adiometer (Delta Ohm HD 2101.2) equipped with an irradiance probe (LP 471 RAD) measured the fluence rate of the dichromatic lamp, with 25 cm between it and the samples. 21.93 mW/cm<sup>2</sup> was the average fluence rate. Aliquots of 1 ml were taken from each petri dish at the start of the experiment and subsequently every 60 min (until 180 min). Serial dilutions were carried out and the pour plate technique was used to monitor cell numbers. Control experiments using uncoated beads and porphyrin-coated beads kept in the dark were performed.

### 3. Results and discussion

**Synthesis and  $^1\text{H}$  NMR spectra.** The syntheses of the thienyl-porphyrins are described in the [Supporting information](#). The

aldehydes were prepared by Sonogashira coupling.<sup>44</sup> Thienyl porphyrins were prepared using a modified version of Lindsey's porphyrin synthesis.<sup>45</sup> Phenyl porphyrins were synthesised using the Alder-Longo method.<sup>46</sup>

Each of the  $\beta$  pyrrolic protons are equivalent and observed as a sharp singlet in their  $^1\text{H}$  NMR spectra ([Figure S1 and S2, Supporting Information](#)), This signal observed at 8.87 ppm for **ZnTPP**, and at 8.98 ppm for the *meso*-phenyl substituted porphyrins (**P6 / P7**), are shifted downfield for the thienyl porphyrins, to 9.07 ppm for **ZnTThP**, 9.21 ppm for **P1 – P3** and 9.13 ppm for **P4** and **P5**. Deshielding of  $\beta$ -pyrrolic protons in thienyl porphyrins was noted earlier,<sup>19,22,47</sup> and is ascribed to an increase in the ring current of the porphyrin macrocycle due to delocalization onto the thienyl units. The  $\beta$ -pyrrolic protons of the 4'-thien-2'-yl substituted porphyrins (**P4 - P5**) show a 0.6 ppm downfield shift with respect to **ZnTThP** and 5'-thien-2'-yl porphyrins (**P1-P3**) show a 0.18 ppm downfield shift. The greater downfield shift of the  $\beta$ -pyrrolic protons in **P1-P3** compared to **P4-P5** is attributed to the increased  $\pi$  conjugation of the *meso* substituents and the porphyrin macrocycle. The thienyl proton signals are a combination of those expected for mono substituted thienyl groups (2- and 3-) and disubstituted thiophene systems (2,5- and 2,4-). The porphyrin ring results in slightly downfield shifted thienyl proton signals. Phenyl ring proton signals are shifted downfield due to the presence of the porphyrin ring. There is no indication of atropisomerism.

**UV–vis absorption spectroscopy.** The  $\lambda_{\text{max}}$  for the Soret and Q absorption bands of all porphyrins reported here are shown in [Table 1](#), together with molar absorptivity and Stokes shift. The UV–vis absorption spectra of **ZnTPP**, **P1**, **P4** and **P7** are given in [Fig. 2](#).

**P1-P3** display the most substantial bathochromic shifts, compared to **ZnTThP** (+10 nm), whereas **P4** and **P5** are largely the same, with an intermediate shift (5–6 nm) for **P6** and **P7**. Substitution of the thiophene group at the 4' position in **P4** and **P5** has little effect on the absorption spectrum. Substitution of the phenyl ring at the para position results in a red-shifted absorption spectrum. Bathochromically shifted porphyrins also exhibit an increased FWHM of the Soret band (**P1-P3** and **P6**, **P7**). The bathochromic shift of the Soret bands increase in the order of: **ZnTPP** < **P7** < **P6** < **ZnTThP** = **P4** < **ZnT3ThP** < **P1** = **P2** = **P3**. The structural similarities between **ZnTPP** and **P6-P7** are consistent with the minor bathochromic shifts in the Soret band due to the nonplanar orientation of the phenyl ring with respect to the porphyrin plane. This arrangement disrupts electronic communication between the thienyl substituents and the porphyrin.<sup>21</sup> **ZnTThP** and **P4** display a similar small bathochromic shift indicating that the phenyl ring does not interact to the same extent as in **P1** due to the position of the substituent. The thienyl groups of **P1-P3** appear to interact similarly with the porphyrin. The co-planar arrangement of the thien-2-yl permits good electronic and vibronic coupling.

The normalized spectra highlight the varied position of the Q-bands. Porphyrins **P1-P3**, **P6**, and **P7** exhibited an increase in the absorptivity of the Q(0,0) band with respect to Q(1,0) when compared to **ZnTThP** and **ZnTPP**, respectively. This increase in absorptivity of the Q-bands was previously observed by Rochford et. al.<sup>15</sup> The Q(0,0) bands increased in the order of **ZnTPP** < **P6** < **ZnTThP** < **P1** < **P2** = **P7** < **ZnT3ThP** < **P4**. In contrast, the absorbance of the Q(1,0) band increased in the order of **ZnTPP** = **ZnTThP** < **P6** < **P2** < **ZnT3ThP** < **P1** < **P4** < **P7**. These results are in agreement with those of Harriman and Fonda, where increased electronic communication between the porphyrin macrocycle and the *meso* substituents resulted in "intensity exchange" of the  $S_2 \leftarrow S_0$  and  $S_1 \leftarrow S_0$  transitions.<sup>48,49</sup>

**Steady-State and Time-Resolved Emission spectroscopy.** As for the absorption spectra, the emission spectra of the porphyrins follow trends dependent on their substitution pattern ([Fig. 3](#)). Porphyrins **P1-P3** exhibit poorly resolved, red-shifted fluorescence bands that arise from emission from the Q(0,0)\* and Q(0,1)\* excited states. The spectra are poorly resolved due to the greater redshift of the Q(0,0)\* band than the Q(0,1)\* band ([Figure S5, Supporting Information](#)) as reported

**Table 1**

Photophysical data of **ZnTPP**, **ZnTThP**, **ZnT3ThP**, *meso*-Zn(II)thien-2'-yl porphyrins (**P1** – **P5**) and *meso*-Zn(II)phenyl porphyrins (**P6** -**P7**) recorded in dichloromethane at room temperature.  $^1\text{O}_2$  quantum yields were measured with respect to **ZnTPP** (430 nm excitation, quantum yield 0.68).

Porphyrin	UV-vis		Q(0,1) $\lambda_{\text{max}}$ nm	Q(0,0) $\lambda_{\text{max}}$ , nm	Emission Fl. Q(0,0)*, (0,1)* $\lambda_{\text{max}}$ , nm	$\Phi_{\text{fl}}$	Stokes shift, ( $\text{cm}^{-1}$ )	$\tau_{\text{fl}}$ , ns	Singlet Oxygen	
	Soret $\lambda_{\text{max}}$ , nm	FWHM ( $\text{cm}^{-1}$ )							$^3\tau$ , $\mu\text{s}$	$^1\text{O}_2$
<b>ZnTPP</b>	419	514	547	588	595, 643	0.13	200	1.8	24	0.68
<b>ZnTThP</b>	429	813	556	600	617, 658	0.12	459	1.4	20	0.48
<b>ZnT3ThP</b>	422	958	551	592	601, 647	0.10	253	1.2	8	0.70
<b>P1</b>	439	1197	559	603	634	0.05	811	0.8	9	0.88
<b>P2</b>	439	1350	559	603	635	0.12	836	0.7	7	0.61
<b>P3</b>	439	1252	559	603	635	0.13	836	0.7	11	0.61
<b>P4</b>	429	870	555	596	613, 652	0.07	465	0.8	36	0.68
<b>P5</b>	425	828	550	590	601, 647	0.18	311	1.4	51	0.54
<b>P6</b>	426	772	550	590	605, 646	0.26	420	1.8	26	–
<b>P7</b>	425	775	550	590	603, 650	0.19	365	1.5	54	0.48

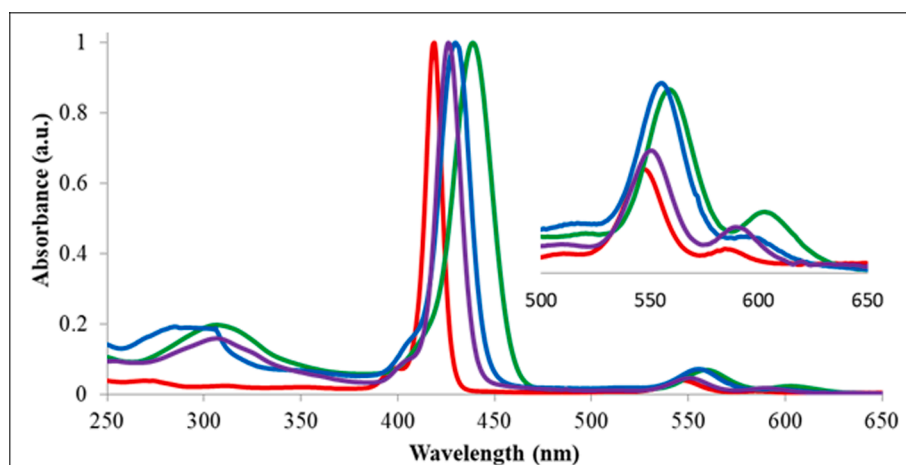


**Fig. 2.** Normalised UV-vis spectra of **ZnTPP** (red), **P1** (green), **P4** (blue) and **P7** (purple) in dichloromethane at room temperature ( $\lambda_{\text{max}} = 1$  AU).

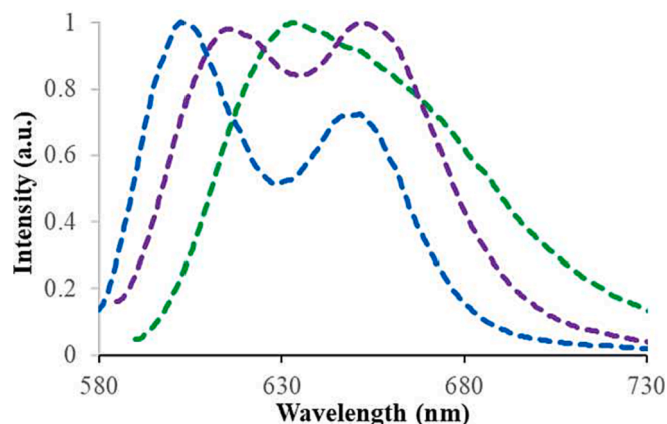


**Fig. 3.** Normalised emission spectra of **P1** (green), **P4** (blue) and **P7** (purple) in dichloromethane at room temperature ( $\lambda_{\text{exc}} = 555$  nm).

earlier for tetra-*meso*(thien-2-yl)porphyrins.<sup>19</sup> There is little difference in the observed Q(0,0)\* and Q(0,1)\* bands of **P4** and **P5** compared to **ZnTThP** (Table 1). The Q(0,0)\* of the phenyl-substituted porphyrins **P6**-**P7**, were bathochromically shifted for the Q(0,0)\* band, however the Q(0,1)\* band remained unchanged (Table 1).

The fluorescence lifetimes ( $\tau_{\text{fl}}$ ) of the porphyrins were considerably shorter than **ZnTPP** (1.83 ns)<sup>50</sup> and **ZnTThP** (Table 1).<sup>1,15</sup> The *meso*-substituent influenced the profile of the emission spectra (see Fig. 4). The shape of the emission spectrum of **P4** is similar to that of **ZnTThP**, and **P6** and **P7** are similar to **ZnT3ThP**. Shorter lifetimes were obtained

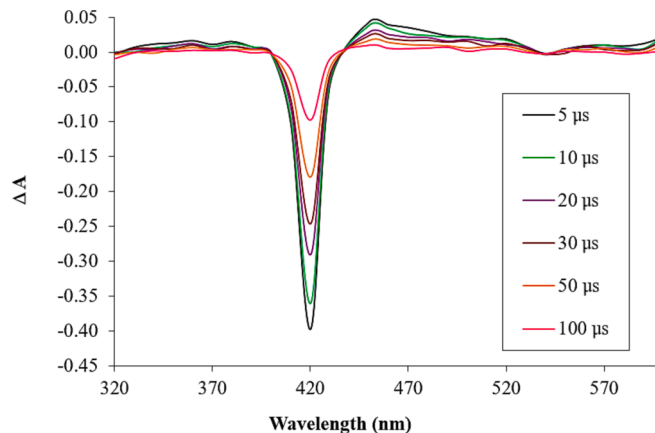


**Fig. 4.** Transient absorbance difference spectra of **P7** in toluene following 355 nm excitation under 1 atm argon.

for the tetra(thien-2'-yl)porphyrins ranging from 0.72 to 1.39 ns with the shortest lifetimes observed for **P2** and **P3** (0.72 ns). In comparison to **ZnTPP**, the fluorescence lifetimes of the tetra(phenyl)porphyrins **P6** and **P7** were shorter (1.56 and 1.47 ns respectively). Shorter fluorescence lifetimes and decreased fluorescence quantum yields have been attributed to the heavy atom effects induced by the sulfur atoms within the thienyl groups,<sup>1,16,20,21</sup> due to greater spin-orbit coupling and enhanced non-radiative decay processes, i.e. intersystem crossing (ISC).<sup>15,16</sup>

<sup>3</sup>( $\pi - \pi^*$ ) Excited State Absorption and Decay. The excited state

transient absorption (TA) difference spectrum of all porphyrins studied, display the expected transient absorption spectra with a maximum between 440 and 500 nm, ascribed to the lowest energy  $^3(\pi-\pi^*)$  triplet excited state of the porphyrin and a depletion in the Soret region due depletion of the porphyrin ground state population. The maximum absorption in the excited state TA spectrum of **ZnTThP** ( $\lambda_{\max} = 490$  nm) was red-shifted relative to **ZnTPP** ( $\lambda_{\max} = 470$  nm). The tetra(thien-2-yl) porphyrins, **P1** – **P5**, also dipalyed bathochromically shifted transient absorbance spectra, compared to with respect to **ZnTPP**. The data corresponded to an earlier report by Rochford et al., where the transient absorption spectra for a series of thien-2-yl porphyrins were also red-shifted when compared to **ZnTPP**.<sup>51</sup> **P7** showed TA spectra like that of **ZnTPP** with a  $\lambda_{\max}$  at 450 nm, and weak TA in the UV region but without significant excited state absorption at longer wavelengths. Triplet lifetimes of 24  $\mu$ s and 20  $\mu$ s, respectively were obtained for **ZnTPP** and **ZnTThP**, which corresponds well with those reported by Rochford and Brücker.<sup>17,51</sup> The triplet lifetime of the novel thienyl porphyrins follow trends previously reported by Nyokong and Manathanath.<sup>14,52</sup> For **P1**–**P3**, triplet lifetimes were shorter than for **ZnTPP** and **ZnTThP** (see Table 1). Both **P4** and **P6** have triplet lifetimes similar to **ZnTPP** and **ZnTThP** (51  $\mu$ s, 54  $\mu$ s). In contrast, both **P5** and **P7** have longer triplet excited state lifetimes at 51  $\mu$ s and 54  $\mu$ s respectively.

As reported by Rochford et al., solvatochromism can indicate enhanced electronic communication by the appearance of a long wavelength fluorescence band in the 580 to 800 nm region.<sup>51</sup> In polar solvents, an increase in intensity of the low-energy band indicates an excited charge transfer transition. The intensity of this low-energy band increased with an increase in solvent polarity (SI), consistent with a charge transfer excited state.

**Cyclic Voltammetry.** The substitution pattern at the *meso* position of the porphyrins in this study was manifested in the redox properties. The half-wave potentials ( $E_{1/2}$ ) at positive potentials (Table 2) correspond to the first and second reversible oxidations of the porphyrin  $\pi$  system, which are assigned to the porphyrin cation radical and porphyrin dication, respectively. All compounds exhibited two redox waves at negative potentials corresponding to the formation of the porphyrin anion radical and dianionic species.

Notably, all the *meso* tetrathien-2-yl porphyrins showed a shift of their first oxidation to more positive potential relative to **ZnTPP**, which indicated stabilization of the HOMO of the porphyrin. Similar characteristics of thienyl porphyrins have been reported previously.<sup>21,51</sup> Positive shifts were observed for **P1**–**P3** (110, 120, 130 mV, respectively) against **ZnTPP** ( $E_{1/2} = +0.78$  vs SCE). Porphyrins **P4** and **P5** were oxidized at the same potential, +0.85 and +0.86 V vs SCE (70 and 80 mV positive shift), respectively, compared to the first oxidation of **ZnTPP**. Stabilization of the HOMO was less pronounced when the *meso* thienyl ring was substituted in the thien-4-yl position. The tetra-phenyl substituted porphyrins (**P6**, 80 mV and **P7**, 70 mV) showed a similar positive shift of their first oxidation with respect to **ZnTPP**. When the phenyl moiety of **ZnTPP** was replaced with that of a *meso*-thienyl group

**Table 2**  
Redox potentials of thienyl porphyrins in dichloromethane (0.1 M TBAPF<sub>6</sub>) vs SCE.  $E_{pa}$  = anodic peak potential.  $E_{pc}$  = cathodic peak potential.

	Oxidation (V)		Reduction (V)			
	1st	2nd	1st	2nd	$E_{1/2}$	$E_{pc}$
<b>ZnTPP</b>	$E_{1/2}$ 0.78	$E_{1/2}$ 1.08	$E_{pc}$ -1.44	$E_{pa}$ -1.38	$E_{1/2}$ -1.41	$E_{pc}$ -1.83
<b>P1</b>	0.89	1.06	-1.19	-1.14	-1.16	-1.36
<b>P2</b>	0.90	1.06	-1.19	-1.16	-1.17	-1.49
<b>P3</b>	0.91	1.06	-1.19	-1.32	-1.26	-1.53
<b>P4</b>	0.85	1.15	-1.36	-1.26	-1.31	-1.70
<b>P5</b>	0.86	1.14	-1.36	-1.28	-1.32	-1.72
<b>P6</b>	0.86	1.13	-1.38	-1.44	-1.41	-1.69
<b>P7</b>	0.85	1.14	-1.38	-1.49	-1.43	-1.71

(**P1**–**P5**), first oxidation potentials were shifted to more positive potentials indicating stabilization of the HOMO ( $a_{2u}$ ) orbital, as reported by Rochford et al.<sup>51</sup>

Thienyl substitution at the 5' position resulted in stabilization of the HOMO whereas *meso*-phenyl substituents in place of a thienyl, stabilized the LUMO, manifested in a shift to less negative potentials of the first reduction. Again **P1** – **P3** showed the largest effect with a decrease in their reduction potential compared to **ZnTPP**. For **P1**, **P2**, and **P3** a reduction of 250 mV, 240 mV and 150 mV were more positive than **ZnTPP**, respectively (**ZnTPP**  $E_{1/2} = -1.41$  vs SCE). Stabilization of the LUMO, was less pronounced for the remainder of the porphyrins examined. Both thienyl porphyrins **P4** and **P5** were shifted by 100 and 90 mV respectively ( $E_{1/2} = -1.31$  V and  $-1.32$  V vs SCE). There was no evident shift in the first reduction of **P6** and only a slight shift to more negative potentials for **P7** ( $E_{1/2} = -1.43$  V vs SCE). The redox data indicate stabilization of both the HOMO and LUMO, which was unexpected as the *meso*-substituents are not co-planar to the porphyrin ring reducing overlap of the  $\pi$ -systems.

**Resonance Raman Spectroscopy.** Resonance Raman spectra recorded at 405 and 473 nm show the expected bands for zinc porphyrins. The 1605  $\text{cm}^{-1}$  band is typical for a phenyl ring and is present in the spectra of **ZnTPP**, **P6**, and **P7** only (Fig. 5). The spectra of the porphyrins are similar despite the bathochromic shift that occurs for thienyl-porphyrins. Compared with **ZnTPP**, the relative intensity at  $\sim 1550$   $\text{cm}^{-1}$  and 1358  $\text{cm}^{-1}$  are similar for all macrocycles. The contribution of modes from substituents at the *meso* position in the porphyrins in the spectra following 473 nm excitation, reflects the electronic delocalization over these moieties. Notably both **P6** and **P7** show resonance enhancement of the peripheral phenyl group showing extended conjugation.

Raman spectra recorded at 473 nm, are resonant with the Q bands and are quite similar to **ZnTPP** in relation to bands at  $\sim 1550$   $\text{cm}^{-1}$  ( $\nu_2$ ),  $\sim 1360$   $\text{cm}^{-1}$  ( $\nu_4$ ) and 1000  $\text{cm}^{-1}$ .

There are significant differences between the Raman spectra of **P6** and **P7** compared to the other porphyrins (see Fig. 7) due to their intense band at  $\sim 1250$   $\text{cm}^{-1}$ . The band at 1250  $\text{cm}^{-1}$  in Fig. 7, was previously reported in the spectra of phenylacetylene porphyrins.<sup>53</sup> Fig. 6 shows structural similarities between **ZnTPP**, **P6**, and **P7** due to the phenyl mode at  $\sim 1600$   $\text{cm}^{-1}$ . The spectra of the other porphyrins are similar to **ZnTThP**, most likely due to the localization of the transition (Soret) on the core of the porphyrin.

**Singlet Oxygen Generation.** The singlet oxygen generation efficiency of the thienyl porphyrins was measured in air-equilibrated dichloromethane against **ZnTPP** by integration of the  $^1\text{O}_2$  emission band at ca. 1260 nm. Within experimental error ( $\pm 5\%$ ), most complexes displayed similar quantum yields for  $^1\text{O}_2$  generation except **P1** and **P7**. The quantum yield for  $^1\text{O}_2$  emission from **P7** (0.48) was similar to **ZnTPP** and substantially lower to that of **P1** despite the triplet life for **P7** being almost twice as long as that of **P1**. This observation has previously been reported by others, with the rationale that energy transfer to generate singlet oxygen may compete with electron transfer to form superoxides.<sup>54</sup>

**Antimicrobial Response.** The antibacterial activity of glass beads coated with **ZnTPP** and the thienyl porphyrin **ZnTThP** was evaluated against *S. aureus* and *E. coli*. Immobilized **ZnTPP** showed good antibacterial activity against *S. aureus* with a 100 % (5 log) reduction in the numbers of *S. aureus* cells following irradiation for 180 min. Antibacterial activity against *E. coli* was also observed albeit that growth inhibition was less pronounced with *E. coli*, and reduced by approximately 50 %. **ZnTThP** also showed good antibacterial activity against *S. aureus* with a 100 % (5 log) reduction in the numbers of *S. aureus* cells following irradiation for 180 min. However, the rate of reduction was greater for **ZnTPP** where nearly an 80 % reduction in cell number was observed after 120 min, while approximately a 50 % reduction in cell number was observed for **ZnTThP** for the same time interval. The difference in response of the two porphyrins is tentatively attributed to the difference

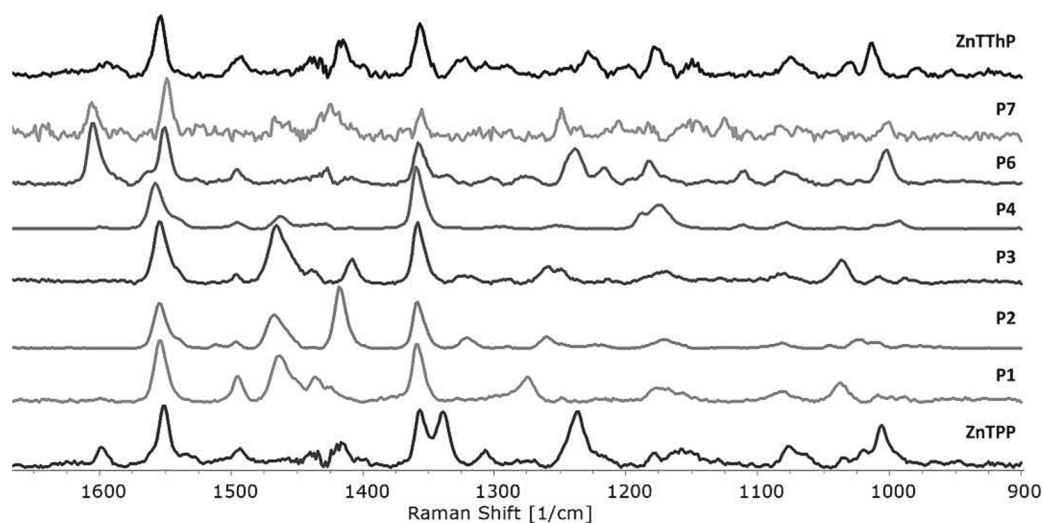


Fig. 5. Raman spectra ( $\lambda_{exc}$  473 nm) of ZnTPP, P1-P4, P6, P7 and ZnT3ThP. Spectra are baseline corrected to remove contributions from fluorescence and solvent bands were removed by scaled subtraction.

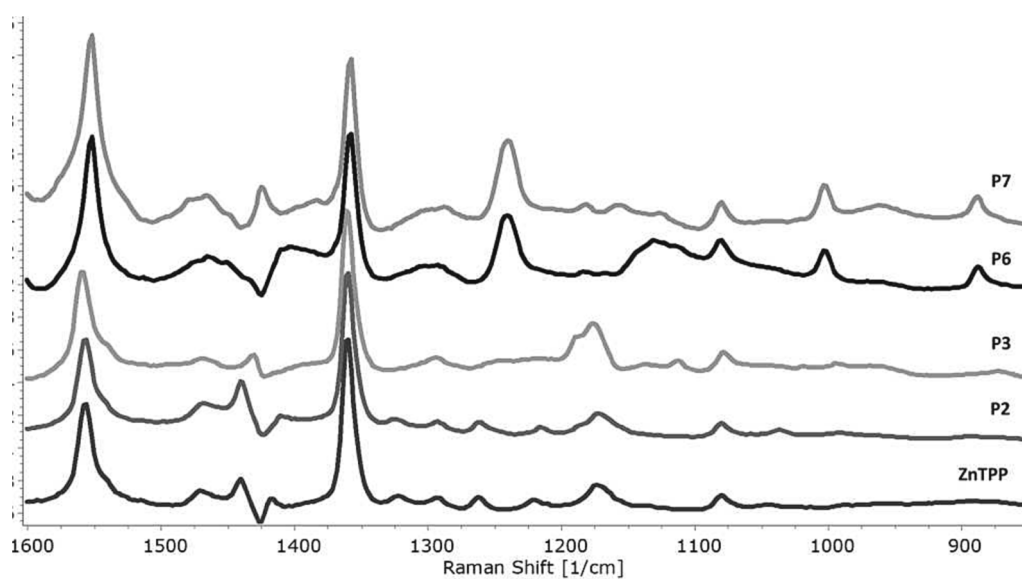


Fig. 6. Raman spectra ( $\lambda_{exc}$  405 nm) of P2, P3, P4, P6 and P7. Spectra are baseline corrected to remove contributions from fluorescence and solvent bands have been removed by scaled subtraction.

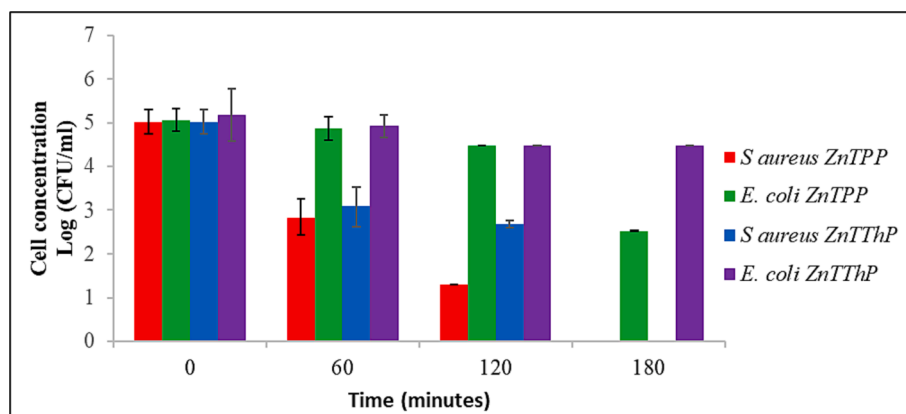


Fig. 7. Bacterial cell concentration of *E. coli* and *S. aureus* in the presence of ZnTPP and ZnTThP coated glass beads. Irradiation was with a dichromatic lamp (430 and 660 nm) for 180 min. Experiments were carried out in triplicate.

in the levels of singlet oxygen generated. Zoltan et al. observed an efficient inactivation of *Escherichia coli* when meso-tetra(pyren-1-yl) porphyrin complexes of Ni(II), Cu(II), and Zn were evaluated against the bacteria, and established a direct relationship between the singlet oxygen quantum yield and antibacterial activity.<sup>55</sup>

**Conclusions.** A series of zinc-chelated thienyl-functionalized porphyrins was synthesised and characterized by photophysical and electrochemical methods. All porphyrins within this series show a bathochromic shift of the Soret band with respect to the porphyrins **ZnTPP**, **ZnTThP** and **ZnT3ThP** due to extended  $\pi$ -conjugation. The photophysical characteristics were dictated by  $\pi$ -conjugation and structural arrangement. The in-planar thienyl ligands (**P1-P3**) exhibited the most extended  $\pi$ -conjugation and electronic coupling. Porphyrin-ligand electronic communication was enhanced by the addition of thienyl moieties and disrupted by the addition of phenyl units between the macrocycle and a thienyl moiety. Additionally, the substituents at the meso-position strongly influenced the shape of the emission spectrum and lifetimes, with the presence of additional thiophene units resulting in shorter fluorescence lifetimes.<sup>25</sup> **ZnTPP** and **ZnTThP** exhibited moderate antibacterial activity towards Gram-positive bacteria (*S. aureus*). Enhanced antibacterial activity was noted for **ZnTPP**, possibly due to the differences in singlet oxygen quantum yield, however, further antimicrobial analyses are required to confirm the mechanism of action.

#### CRedit authorship contribution statement

**Jessica S.O. Neill:** Investigation, Data curation, Writing - original draft, Writing - review & editing. **Nicola M. Boyle:** Formal analysis, Data curation, Writing - original draft. **Katharina Heintz:** Methodology, Investigation, Formal analysis, Writing - review & editing. **Wesley R. Browne:** Conceptualization, Methodology, Writing - original draft, Writing - review & editing. **Brid Quilty:** Formal analysis, Conceptualization, Writing - review & editing. **Mary T. Pryce:** Supervision, Conceptualization, Funding acquisition, Project administration, Writing - original draft, Writing - review & editing.

#### Declaration of Competing Interest

The authors declare that they have no known competing financial interests or personal relationships that could have appeared to influence the work reported in this paper.

#### Data availability

Data will be made available on request.

#### Acknowledgements

The authors gratefully acknowledge financial funding provided by the Sustainable Energy Authority of Ireland (under the SEAI National Energy Research, Development & Demonstration Funding Programme 2018, Grant number 18/RDD/282), Dublin City University for a scholarship (NMB) and from SFI (19/FFP/6882).

#### Appendix A. Supplementary data

Supplementary data to this article can be found online at <https://doi.org/10.1016/j.jphotochem.2023.114573>.

#### References

- N.M. Boyle, J. Rochford, M.T. Pryce, Thienyl-Appended Porphyrins: Synthesis, Photophysical and Electrochemical Properties, and Their Applications, *Coordination Chemistry Reviews*. Elsevier January 1 254 (1-2) (2010) 77–102.
- A. Vasilev, A. Kostadinov, M. Kandinska, K. Landfester, S. Balushev, Tetrathienothiophene Porphyrin as a Metal-Free Sensitizer for Room-Temperature

- Triplet-Triplet Annihilation Upconversion, *Front Chem* 10 (2022), <https://doi.org/10.3389/FCHEM.2022.809863>.
- B. Babu, A. Sindelo, J. Mack, T. Nyokong, Thien-2-Yl Substituted Chlorins as Photosensitizers for Photodynamic Therapy and Photodynamic Antimicrobial Chemotherapy, *Dyes and Pigments* 185 (2021), 108886, <https://doi.org/10.1016/J.DYEPIG.2020.108886>.
- Y. Wang, L. Xu, X. Wei, X. Li, H. Agren, W. Wu, Y. Xie, 2-Diphenylaminothiophene as the Donor of Porphyrin Sensitizers for Dye-Sensitized Solar Cells, *New Journal of Chemistry* 38 (7) (2014) 3227–3235, <https://doi.org/10.1039/c4nj00651h>.
- J. Ramesh, C. Arunkumar, S. Sujatha, A. B. Porphyrins Bearing Thienyl/Pyridyl Moieties Obtained via Scrambling: Characterization, DNA Interaction and Anticancer Studies. *ChemistrySelect* 3 (37) (2018) 10468–10474, <https://doi.org/10.1002/slct.201802068>.
- J. Ramesh, C. Arunkumar, S. Sujatha, Dicationic Porphyrins Bearing Thienyl and Pyridinium Moieties: Synthesis, Characterization, DNA Interaction and Cancer Cell Toxicity, *Polyhedron* 170 (2019) 151–159, <https://doi.org/10.1016/j.poly.2019.05.042>.
- J. Shipp, S. Parker, S. Spall, S.L. Peralta-Arriaga, C.C. Robertson, D. Chekulaev, P. Portius, S. Turega, A. Buckley, R. Rothman, J.A. Weinstein, Photocatalytic Reduction of CO<sub>2</sub> to CO in Aqueous Solution under Red-Light Irradiation by a Zn-Porphyrin-Sensitized Mn(I) Catalyst, *Inorg Chem* 61 (34) (2022) 13281–13292, <https://doi.org/10.1021/ACS.INORGCHEM.2C00091>.
- J.D.B. Koenig, J. Willkomm, R. Roesler, W.E. Piers, G.C. Welch, Electrocatalytic CO<sub>2</sub> Reduction at Lower Overpotentials Using Iron(III) Tetra(Meso-Thienyl) Porphyrins, *ACS Appl Energy Mater* 2 (6) (2019) 4022–4026, <https://doi.org/10.1021/acsaeam.9b00761>.
- S.M. Shabangu, B. Babu, R.C. Soy, J. Oyim, E. Amuhaya, T. Nyokong, Susceptibility of *Staphylococcus Aureus* to Porphyrin-Silver Nanoparticle Mediated Photodynamic Antimicrobial Chemotherapy, *J Lumin* 222 (2020), 117158, <https://doi.org/10.1016/j.jlumin.2020.117158>.
- M. Luciano, M. Erfanzadeh, F. Zhou, H. Zhu, T. Bornhütter, B. Röder, Q. Zhu, C. Brückner, In Vivo Photoacoustic Tumor Tomography Using a Quinoline-Annulated Porphyrin as NIR Molecular Contrast Agent, *Org Biomol Chem* 15 (4) (2017) 972–983, <https://doi.org/10.1039/C6OB02640K>.
- M. Taniguchi, J.S. Lindsey, D.F. Bocian, D. Holten, Comprehensive Review of Photophysical Parameters ( $\epsilon$ ,  $\Phi_f$ ,  $\tau_s$ ) of Tetraphenylporphyrin (H2TPP) and Zinc Tetraphenylporphyrin (ZnTPP) – Critical Benchmark Molecules in Photochemistry and Photosynthesis, *Journal of Photochemistry and Photobiology C: Photochemistry Reviews* 46 (2021), 100401, <https://doi.org/10.1016/J.JPHOTOCHEMREV.2020.100401>.
- S. Yang, L. Liu, Z. Jia, D. Jia, Y. Luo, Structure and Mechanical Properties of Rare-Earth Complex La-GDTC Modified Silica/SBR Composites, *Polymer (Guildf)* 52 (12) (2011) 2701–2710, <https://doi.org/10.1016/j.polymer.2011.04.015>.
- X. Zhang, Y. Zhu, X. Wu, H. He, G. Wang, Q. Li, Meso-Schiff-Base Substituted Porphyrin Dimer Dyes for Dye-Sensitized Solar Cells: Synthesis, Electrochemical, and Photovoltaic Properties, *Research on Chemical Intermediates* 41 (7) (2015) 4227–4241, <https://doi.org/10.1007/s11164-013-1525-1>.
- B. Babu, E. Amuhaya, D. Oluwale, E. Prinsloo, J. Mack, T. Nyokong, Preparation of NIR Absorbing Axial Substituted Tin(IV) Porphyrins and Their Photocytotoxic Properties, *Medchemcomm* 10 (1) (2019) 41–48, <https://doi.org/10.1039/C8MD00373D>.
- J. Rochford, A.D. Rooney, M.T. Pryce, Redox Control of Meso-Zinc(II) Ferrocenylporphyrin Based Fluorescence Switches, *Inorg Chem* 46 (18) (2007) 7247–7249, <https://doi.org/10.1021/ic0703326>.
- X. Zhang, S. Abid, L. Shi, Z. Sun, O. Mongin, M. Blanchard-Desce, F. Paul, C. O. Paul-Roth, New Conjugated Meso-Tetrathienylporphyrin-Cored Derivatives as Two-Photon Photosensitizers for Singlet Oxygen Generation, *Dyes and Pigments* 153 (2018) 248–255, <https://doi.org/10.1016/J.DYEPIG.2018.01.028>.
- C. Brückner, P.C.D. Foss, J.O. Sullivan, R. Pelto, M. Zeller, R.R. Birge, G. Crundwell, Origin of the Bathochromically Shifted Optical Spectra of Meso-Tetrathienyl-2'- and 3'-Ylporphyrins as Compared to Meso-Tetraphenylporphyrin, *Phys Chem Chem Phys* 8 (20) (2006) 2402–2412, <https://doi.org/10.1039/B600010J>.
- J.S. O'Neill, L. Kearney, M.P. Brandon, M.T. Pryce, Design Components of Porphyrin-Based Photocatalytic Hydrogen Evolution Systems: A Review, *Coord Chem Rev* 467 (2022) 214599.
- X. Sun, J. Zhang, B. He, The Synthesis and Photochemical Characterization of Meso-Tetra-Thienyl Porphyrins, *J Photochem Photobiol A Chem* 172 (2005) 283–288, <https://doi.org/10.1016/j.jphotochem.2004.12.016>.
- P.R. Kumar, N.J. Britto, A. Kathiravan, A. Neels, M. Jaccob, E.M. Mothi, Synthesis and Electronic Properties of A3B-Thienyl Porphyrins: Experimental and Computational Investigations, *New Journal of Chemistry* 43 (3) (2019) 1569–1580, <https://doi.org/10.1039/C8NJ04289F>.
- A. Ghosh, S.M. Mobin, R. Fröhlich, R.J. Butcher, D.K. Maity, M. Ravikanth, Effect of Five Membered versus Six Membered Meso-Substituents on Structure and Electronic Properties of Mg(II) Porphyrins: A Combined Experimental and Theoretical Study, *Inorg Chem* 49 (18) (2010) 8287–8297, <https://doi.org/10.1021/ic1008522>.
- I. Gupta, M. Ravikanth, Spectroscopic Properties of Meso-Thienylporphyrins with Different Porphyrin Cores, *J Photochem Photobiol A Chem* 177 (2-3) (2006) 156–163, <https://doi.org/10.1016/j.jphotochem.2005.05.020>.
- J.-H. Ha, S. Ko, C.-H. Lee, W.-Y. Lee, Y.-R. Kim, Effect of Core Atom Modification on Photophysical Properties and Singlet Oxygen Generation Efficiencies, Tetraphenylporphyrin Analogues Core-Modified by Oxygen and/or Sulfur 349 (3-4) (2001) 271–278.

- [24] J.M.S. Lopes, J.R.T. Reis, A.E.H. Machado, T.H.O. Leite, A.A. Batista, T.V. Acunha, B.A. Iglesias, P.T. Araujo, N.M. Barbosa Neto, Influence of the Meso-Substituents on the Spectral Features of Free-Base Porphyrin, *Spectrochim Acta A Mol Biomol Spectrosc* 238 (2020) 118389.
- [25] R. Ambre, K.B. Chen, C.F. Yao, L. Luo, E.W.G. Diau, C.H. Hung, Effects of Porphyrinic Meso-Substituents on the Photovoltaic Performance of Dye-Sensitized Solar Cells: Number and Position of p-Carboxyphenyl and Thienyl Groups on Zinc Porphyrins, *Journal of Physical Chemistry C* 116 (22) (2012) 11907–11916, <https://doi.org/10.1021/jp302145x>.
- [26] B. Purushothaman, B. Varghese, P. Bhyrappa, [5,10,15,20-Tetrakis(2-Thienyl)-Porphyrinato]Zinc(II), *Acta Crystallogr C* 57 (3) (2001) 252–253, <https://doi.org/10.1107/S0108270100018552>.
- [27] S.M. Shabangu, B. Babu, R.C. Soy, M. Managa, K.E. Sekhosana, T. Nyokong, Photodynamic Antimicrobial Chemotherapy of Asymmetric Porphyrin-Silver Conjugates towards Photoinactivation of *Staphylococcus Aureus*, *J Coord Chem* 73 (4) (2020) 593–608, <https://doi.org/10.1080/00958972.2020.1739273>.
- [28] D. Mathew, J. Ramesh, S. Sasidharan, K. Subburaj, P. Saudagar, P. Parameswaran, S. Sujatha, Synthesis, TDDFT Calculations and Biological Evaluation of Dicationic Porphyrins as Groove Binders and Antimicrobial Agents, *ChemistrySelect* 6 (3) (2021) 396–409, <https://doi.org/10.1002/SLCT.202003858>.
- [29] K. Alenezi, A. Tovmasyan, I. Batinic-Haberle, L.T. Benov, Optimizing Zn Porphyrin-Based Photosensitizers for Efficient Antibacterial Photodynamic Therapy, *Photodiagnosis Photodyn Ther* 17 (2017) 154–159, <https://doi.org/10.1016/j.pdpdt.2016.11.009>.
- [30] A. Galstyan, Y.K. Maurya, H. Zhilytskaya, Y.J. Bae, Y.-L. Wu, M.R. Wasielewski, T. Lis, U. Dobrindt, M. Stepień,  $\Pi$ -Extended Donor-Acceptor Porphyrins and Metalloporphyrins for Antimicrobial Photodynamic Inactivation. *Chemistry – A, European Journal* 26 (37) (2020) 8262–8266.
- [31] M.H. Staegemann, B. Gitter, J. Dernerde, C. Kuehne, R. Haag, A. Wiehe, Mannose-Functionalized Hyperbranched Polyglycerol Loaded with Zinc Porphyrin: Investigation of the Multivalency Effect in Antibacterial Photodynamic Therapy, *Chemistry – A European Journal* 23 (16) (2017) 3918–3930, <https://doi.org/10.1002/chem.201605236>.
- [32] Hilmey, D. G.; Abe, M.; Nelen, M. I.; Stilts, C. E.; Baker, G. A.; Baker, S. N.; Bright, F. V.; Davies, S. R.; Gollnick, S. O.; Oseroff, A. R.; Gibson, S. L.; Hilf, R.; Detty, M. R. Water-Soluble, Core-Modified Porphyrins as Novel, Longer-Wavelength-Absorbing Sensitizers for Photodynamic Therapy. II. Effects of Core Heteroatoms and Meso-Substituents on Biological Activity. *J Med Chem* 2002, 45 (2), 449–461. 10.1021/jm0103662.
- [33] C.P. Hsieh, H.P. Lu, C.L. Chiu, C.W. Lee, S.H. Chuang, C.L. Mai, W.N. Yen, S.J. Hsu, E.W.G. Diau, C.Y. Yeh, Synthesis and Characterization of Porphyrin Sensitizers with Various Electron-Donating Substituents for Highly Efficient Dye-Sensitized Solar Cells, *J Mater Chem* 20 (6) (2010) 1127–1134, <https://doi.org/10.1039/B919645E/>.
- [34] Kumar, P. R.; Shajan, X. S.; Mothi, E. M. Pyridyl/Hydroxyphenyl versus Carboxyphenyl Anchoring Moieties in Zn - Thienyl Porphyrins for Dye Sensitized Solar Cells. *Spectrochim Acta A Mol Biomol Spectrosc* 2020, 224. 10.1016/J.SAA.2019.117408.
- [35] Fernández, L.; Esteves, V. I.; Cunha, A.; Schneider, R. J.; Tomé, J. P. C. Photodegradation of Organic Pollutants in Water by Immobilized Porphyrins and Phthalocyanines. *10.1142/S108842461630007X* 2016, 20 (1–4), 150–166. 10.1142/S108842461630007X.
- [36] M.C. DeRosa, R.J. Crutchley, Photosensitized Singlet Oxygen and Its Applications, *Coord Chem Rev* 233–234 (2002) 351–371, [https://doi.org/10.1016/S0010-8545\(02\)00034-6](https://doi.org/10.1016/S0010-8545(02)00034-6).
- [37] G. Bertoloni, N. Cazzador, R. Fontana, ULTRASTRUCTURAL FEATURES OF CELL-WALL GROWTH IN PENICILLIN-TREATED BACTERIA, *Caryologia* 35 (1) (1982) 152–153.
- [38] Z. Dai, L. Tian, Y. Xiao, Z. Ye, R. Zhang, J. Yuan, A Cell-Membrane-Permeable Europium Complex as an Efficient Luminescent Probe for Singlet Oxygen, *J Mater Chem B* 1 (7) (2013) 924–927, <https://doi.org/10.1039/c2tb00350c>.
- [39] T.J. Silhavy, D. Kahne, S. Walker, *The Bacterial Cell Envelope. Cold Spring Harbor perspectives in biology*, Cold Spring Harbor Laboratory Press, May 1, 2010,, p. a000414.
- [40] J.L. Alves, B. Revil-Baudard, O. Cazacu, Importance of the Coupling between the Sign of the Mean Stress and the Third Invariant on the Rate of Void Growth and Collapse in Porous Solids with a von Mises Matrix, *Model Simul Mat Sci Eng* 22 (2) (2014), 025005, <https://doi.org/10.1088/0965-0393/22/2/025005>.
- [41] S. Banfi, E. Caruso, L. Buccafurni, V. Battini, S. Zazzaron, P. Barbieri, V. Orlandi, Antibacterial Activity of Tetraaryl-Porphyrin Photosensitizers: An In Vitro Study on Gram Negative and Gram Positive Bacteria, *J Photochem Photobiol B* 85 (1) (2006) 28–38, <https://doi.org/10.1016/j.jphotobiol.2006.04.003>.
- [42] R. Rahimi, F. Fayyaz, M. Rassa, M. Rabbani, Microwave-Assisted Synthesis of 5,10,15,20-Tetrakis(4-Nitrophenyl)Porphyrin and Zinc Derivative and Study of Their Bacterial Photoinactivation. *Iranian Chemical, Communication* (2016).
- [43] J. Mosinger, K. Lang, P. Kubát, J. Sýkora, M. Hof, L. Plíštil, B. Mosinger, Photofunctional Polyurethane Nanofabrics Doped by Zinc Tetraphenylporphyrin and Zinc Phthalocyanine Photosensitizers, *J Fluoresc* 19 (4) (2009) 705–713, <https://doi.org/10.1007/S10895-009-0464-0/FIGURES/9>.
- [44] K. Sonogashira, Y. Tohda, N. Hagihara, A Convenient Synthesis of Acetylenes: Catalytic Substitutions of Acetylenic Hydrogen with Bromoalkenes, Iodoarenes and Bromopyridines. *Tetrahedron Lett* 16 (50) (1975) 4467–4470, [https://doi.org/10.1016/S0040-4039\(00\)91094-3](https://doi.org/10.1016/S0040-4039(00)91094-3).
- [45] J.S. Lindsey, *The Synthesis of Meso-Substituted Porphyrins*, Springer, Dordrecht, 1994, pp. 49–86.
- [46] A.D. Adler, F.R. Longo, W. Shergalis, Mechanistic Investigations of Porphyrin Syntheses. I. Preliminary Studies on Ms-Tetraphenylporphyrin, *J Am Chem Soc* 86 (15) (1964) 3145–3149, <https://doi.org/10.1021/ja01069a035>.
- [47] I. Gupta, C.-H. Hung, M. Ravikanth, Synthesis and Structural Characterization of meso-Thienyl Core-Modified Porphyrins, *European J Org Chem* 2003 (22) (2003) 4392–4400, <https://doi.org/10.1002/ejoc.200300228>.
- [48] A. Harriman, J. Davila, Spectroscopic Studies of Some Zinc Meso-Tetraaryl Porphyrins, *Tetrahedron* 45 (15) (1989) 4737–4750, [https://doi.org/10.1016/S0040-4020\(01\)85149-8](https://doi.org/10.1016/S0040-4020(01)85149-8).
- [49] H.N. Fonda, J.V. Gilbert, R.A. Cormier, J.R. Sprague, K. Kamioka, J.S. Connolly, Spectroscopic, Photophysical, and Redox Properties of Some Meso-Substituted Free-Base Porphyrins, *Journal of Physical Chemistry* 97 (27) (1993) 7024–7033, <https://doi.org/10.1021/j100129a017>.
- [50] Azenha, E. G.; Serra, A. C.; Pineiro, M.; Pereira, M. M.; Seixas de Melo, J.; Arnaud, L. G.; Formosinho, S. J.; Rocha Gonçalves, A. M. d. A Heavy-Atom Effects on Metalloporphyrins and Polyhalogenated Porphyrins. *Chem Phys* 2002, 280 (1–2), 177–190. 10.1016/S0301-0104(02)00485-8.
- [51] J. Rochford, S. Botchway, J.J. McGarvey, A.D. Rooney, M.T. Pryce, Photophysical and Electrochemical Properties of Meso-Substituted Thien-2-Yl Zn(II) Porphyrins, *Journal of Physical Chemistry A* 112 (46) (2008) 11611–11618, <https://doi.org/10.1021/jp805809p>.
- [52] M. Manathanath, M. Xie, C. Arunkumar, Z. Wang, J. Zhao, S. Sujatha, Synthesis, Photophysical, Electrochemical and Photoluminescent Oxygen Sensing Studies of Trans-Pt(II)-Porphyrins, Dyes and Pigments 165 (2019) 117–127, <https://doi.org/10.1016/j.dyepig.2019.02.016>.
- [53] J. Seth, V. Palaniappan, D.F. Bocian, T.E. Johnson, S. Prathapan, J.S. Lindsey, Investigation of Electronic Communication in Multi-Porphyrin Light-Harvesting Arrays, *J Am Chem Soc* 116 (23) (1994) 10578–10592, [https://doi.org/10.1021/JA00102A027/ASSET/JA00102A027.FP.PNG\\_V03](https://doi.org/10.1021/JA00102A027/ASSET/JA00102A027.FP.PNG_V03).
- [54] D.R. Subedi, R. Reid, P.F. D'Souza, V.N. Nesterov, F. D'Souza, Singlet Oxygen Generation in Peripherally Modified Platinum and Palladium Porphyrins: Effect of Triplet Excited State Lifetimes and Meso-Substituents on  $^{1}O_2$  Quantum Yields, *Chemphyschem* 87 (4) (2022) e202200010.
- [55] T. Zoltan, F. Vargas, C. Rivas, V. López, J. Perez, A. Biasutto, Synthesis, Photochemical and Photoinduced Antibacterial Activity Studies of Meso-Tetra (Pyren-1-Yl)Porphyrin and Its Ni, Cu and Zn Complexes. *Sci Pharm* 78 (4) (2010) 767–789, <https://doi.org/10.3797/scipharm.1003-13>.